Modification of Classical Neurochemical Markers in Identified Primary Afferent Neurons With Aβ-, Aδ-, and C-Fibers After Chronic Constriction Injury in Mice

RUTH RUSCHEWEYH, LIESBETH FORSTHUBER, DORIS SCHOFFNEGGER,
AND JÜRGEN SANDKÜHLER*

Department of Neurophysiology, Center for Brain Research, Medical University of Vienna,
A-1090 Vienna, Austria

ABSTRACT

It is functionally important to differentiate between primary afferent neurons with A-fibers, which are nociceptive or nonnociceptive, and C-fibers, which are mainly nociceptive. Neurochemical markers such as neurofilament 200 (NF200), substance P (SP), and isolectin B4 (IB4) have been useful to distinguish between A- and C-fiber neurons. However, the expression patterns of these markers change after peripheral nerve injury, so that it is not clear whether they still distinguish between fiber types in models of neuropathic pain. We identified neurons with Aβ-, Aδ-, and C-fibers by their conduction velocity (corrected for utilization time) in dorsal root ganglia taken from mice after a chronic constriction injury (CCI) of the sciatic nerve and control mice, and later stained them for IB4, SP, calcitonin gene-related peptide (CGRP), NF200, and neuropeptide Y (NPY). NF200 remained a good marker for A-fiber neurons, and IB4 and SP remained good markers for C-fiber neurons after CCI. NPY was absent in controls but was expressed in A-fiber neurons after CCI. After CCI, a group of C-fiber neurons emerged that expressed none of the tested markers. The size distribution of the markers was investigated in larger samples of unidentified dorsal root ganglion neurons and, together with the results from the identified neurons, provided only limited evidence for the expression of SP in Aβ-fiber neurons after CCI. The extent of up-regulation of NPY showed a strong inverse correlation with the degree of heat hyperalgesia. J. Comp. Neurol. 502:325–336, 2007. © 2007 Wiley-Liss, Inc.

Indexing terms: nociception; dorsal root ganglion; peripheral nerve injury; substance P; isolectin B4; neuropathic pain

Sensory information reaches the spinal cord through three major classes of primary afferents, which have their cell bodies in the dorsal root ganglia (DRGs): neurons with thickly myelinated, fast conducting Aα/β-fibers; neurons with thinly myelinated, slower conducting Aδ-fibers; and neurons with unmyelinated, slowly conducting C-fibers. This classification is functionally important because about 90% of the neurons with C-fibers and 70% of the neurons with Aδ-fibers are nociceptors, whereas >80% of the neurons with Aβ-fibers conduct nonnociceptive information (Julius and Basbaum, 2001; Hunt and Mantyh, 2001; Fang et al., 2005). The three fiber types can be distinguished electrophysiologically by their conduction velocity and activation threshold for electrical stimulation. How-

ever, this method is time consuming and, when combined with histochemistry, requires filling and subsequent re-identification of the cell bodies in the DRG. Neurons with

The Journal of Comparative Neurology. DOI 10.1002/cne

326   R. RUSCHEWEYH ET AL.

C-fibers tend to have smaller cell bodies than those with A-fibers, but size is not a reliable indicator, insofar as the overlap between neurons with A- and C-fibers is extensive (see, e.g., Harper and Lawson, 1985). Some neurochemical markers are able to distinguish between neurons with A- and C-fibers. For example, neurofilament 200 (NF200) is limited to neurons with A-fibers in the rat (Lawson and Waddell, 1991). C-fiber neurons can be divided into two, possibly overlapping groups, those that bind isolectin B4 (IB4) and the peptidergic neurons that express substance P (SP) and/or calcitonin gene-related peptide (CGRP; Hunt and Mantyh, 2001). IB4 and SP are quite specific indicators for C-fiber neurons in rat and mouse (McCarthy and Lawson, 1989, 1997; Wang et al., 1994; Dirajlal et al., 2003), whereas CGRP is expressed by all types of primary afferents in the rat (McCarthy and Lawson, 1990; Lawson et al., 1996). These markers have been useful in histochemical studies on DRG neurons in naïve animals, but it is not clear whether they also distinguish between fiber types in animal models of neuropathic pain, in that both their overall expression and their distribution among neurons of different sizes are profoundly affected by peripheral nerve injury in rats and mice (Honoré et al., 2000; Wang et al., 2003; Hammond et al., 2004). Here, we studied the expression of NF200, IB4, SP, and CGRP in electrophysiologically identified Aβ-, Aδ-, and C-fiber neurons in L4 and L5 DRGs taken from mice showing neuropathic pain after a chronic constriction injury (CCI) of the sciatic nerve (Bennett and Xie, 1988). In naïve animals, so far there is no marker able to distinguish between Aβ- and Aδ-fiber neurons. Neuropeptide Y (NPY) is up-regulated selectively in large DRG neurons after peripheral nerve injury in the rat (Wakisaka et al., 1992), and we hypothesized that it might be a marker of neurons with Aβ-fibers in neuropathic animals. Results of the identified neurons were compared with the overall and size distribution of these markers in larger samples of unidentified neurons from the same DRGs.

MATERIALS AND METHODS
Neuropathic animal model and behavioral testing

All animal experiments were in accordance with European Communities Council directives (86/609/EEC) and were approved by the Austrian Federal Ministry for Education, Science and Culture. A CCI model (Bennett and Xie, 1988) modified according to Sommer and Schäfers (1998) was used to induce neuropathic pain in male adult FVB mice [friend virus B-type, obtained from The Jackson Laboratory (Bar Harbor, ME) and interbred at a local facility]. Briefly, mice were deeply anesthetized with isoflurane (1.2–1.5%), and the left sciatic nerve was exposed at midthigh. Proximal to its trifurcation, an ~8-mm portion of the nerve was freed of adhering tissue, and three loose ligatures were tied around the nerve with 7-0 prolene thread at a spacing of ~1 mm. The incision was then closed in two layers, and anesthesia was discontinued. Sham treatment consisted of exposing the nerve without application of the ligatures. Animals were monitored daily and fed and drank normally.

Mechanical and thermal withdrawal thresholds of both hindpaws were tested on the 2 days before the operation and every second day after the operation. Nociceptive mechanical thresholds were evaluated by using a set of von Frey monofilaments of incremental stiffness (Stoelting, Wood Dale, IL). Mice were placed in a transparent cage on a wire mesh floor, and von Frey hairs were applied perpendicularly to the sole of the paw. A brisk withdrawal in response to the stimulus was considered as positive reaction. The first hair presented was the 0.6 g hair. The up-and-down method of Dixon (1965) was used, meaning that, after a negative response, the next stiffer hair was applied, and, after a positive response, the next less stiff hair. Six responses were recorded per session and paw, and the 50% withdrawal threshold was calculated by the method of Chaplan et al. (1994). Mechanical allodynia (pain evoked by normally not painful stimuli) was detected as a significant reduction of mechanical withdrawal thresholds. Nociceptive thermal thresholds were measured according to Hargreaves et al. (1988) by using the plantar test (Ugo Basile, Comerio, Italy). Mice were placed in a cage on a transparent floor, and radiant heat coming from a mobile source was focused onto the sole of one hindpaw. The withdrawal latency was automatically determined by a built-in timer. Three responses were recorded per session and paw. Thermal hyperalgesia (exaggerated reaction to painful stimuli) was detected as a significant reduction of thermal withdrawal latencies.

Recording of compound action potentials

Naïve and neuropathic (days 9–12 after CCI) mice were deeply anesthetized with isoflurane and killed by decapitation. Sciatic nerves (from the trifurcation to the entrance into the spine) were prepared and kept in incubation solution (in mM: NaCl 95, KCl 1.8, KH_2PO_4 1.2, $CaCl_2$ 0.5, $MgSO_4$ 7, $NaHCO_3$ 26, glucose 15, sucrose 50, oxygenated with 95% O_2, 5% CO_2; pH 7.4, measured osmolality 310–320 mOsmol) at room temperature. The nerve segment containing the ligatures was removed, where applicable. For recording of compound action potentials, one nerve was transferred into the recording chamber, where it was superfused with recording solution (identical to incubation solution, except for NaCl 127 mM, $CaCl_2$ 2.4 mM, $MgSO_4$ 1.3 mM, and sucrose 0 mM) at 3 ml/minute and room temperature. The distal end was led into a suction electrode connected to a constant-current stimulator (A320; WPI, Sarasota, FL). The proximal end was led into a second suction electrode connected to an amplifier (Iso-Dam-D; WPI). Compound action potentials evoked by single pulse stimulation (0.1 msec, 0.01–3 mA) were amplified ×100, bandpass filtered at 0.1 Hz to 3 kHz, digitized at 10 kHz, and stored in a computer using the pClamp 8 acquisition software (Molecular Devices, Union City, CA).

The (uncorrected) conduction velocity was calculated from the length of the stimulated nerve segment (distance between stimulation and recording electrode) and the latency from the onset of the stimulation to the onset of the respective compound action potential. The maximum length of the sciatic nerve segment in this preparation was ~20 mm. Each nerve was successively shortened from the distal end to obtain compound action potentials at nerve lengths between 5 and 20 mm. This allowed calculation of the utilization time and consequently of corrected conduction velocities (see Results).

The Journal of Comparative Neurology. DOI 10.1002/cne

PRIMARY AFFERENT MARKERS AFTER NERVE INJURY   327

Intracellular recording and filling of DRG neurons

Naïve, sham operated and neuropathic (day 9–12 after operation) mice were deeply anesthetized with isoflurane and killed by decapitation. The spine and adherent thighs were removed to ice-cold incubation solution. The sciatic nerve was identified at midthigh and followed to the spine. The spine was then opened on the ventral side, and the L4 and L5 DRGs with adhering sciatic nerve and dorsal roots were dissected. In neuropathic and sham-operated mice, only the DRGs ipsilateral to the operation were used, and, in neuropathic animals, the sciatic nerve was cut proximal to the ligatures. The capsule of the DRG was carefully removed with microscissors. The L4 spinal nerve was then cut at the L4/L5 bifurcation of the sciatic nerve, and the L5 ganglion was left in continuity with the sciatic nerve. The preparations were incubated with fura-2 AM (10 μM) and pluronic F-127 (0.02%; both from Molecular Probes, Leiden, The Netherlands) in incubation solution for 90 minutes at room temperature, followed by a washout period of ≥30 minutes.

For recording, the DRG was glued to the bottom of the recording chamber (cyanoacrylate superglue) and superfused with recording solution at 3 ml/minute and room temperature. The peripheral nerve was inserted into a suction electrode connected to a stimulator. The DRG was inspected for vitality of its neurons under an upright microscope (BX50WI; Olympus, Tokyo, Japan) that was equipped with Dodt-infrared optics (Dodt and Zieglgänsberger, 1990) and connected to a cooled CCD camera (TILL Photonics, Gräfeling, Germany). Ca^{2+} imaging was performed by taking paired exposures at 340 and 380 nm at 2 Hz frame rate using a monochromator (TILL Photonics) and calculating the ratio F340/F380 (TILL Vision software package). Neurons in the superficial layer of the DRG that reacted with a Ca^{2+} rise to supramaximal stimulation of the peripheral nerve (0.5 msec, 3 mA, at 100 Hz for 1 second) were selected for intracellular recording. This avoided impalement and accidental dye injection into neurons that did not react to sciatic nerve stimulation.

Selected neurons were impaled under video microscopic guidance with microelectrodes (pulled from filament glass; A-M Systems, Carlsborg, WA) that had tip resistances of 150–300 MΩ when filled with 1% Lucifer yellow (LY; Fluka, Buchs, Switzerland) in 0.5 M LiCl. Current-clamp recordings were made with an Axoclamp 2B amplifier and the pClamp 9 acquisition software (both from Molecular Devices). Signals were lowpass filtered at 10 kHz, digitized at 20 kHz, and analyzed offline in pClamp 9. For each neuron, the response to single-shock stimulation (0.1 msec, 0.01–5 mA) of the sciatic nerve was recorded, and the threshold intensity to elicit an action potential was determined to allow its classification as an Aβ-, Aδ-, or C-fiber neuron. Membrane potentials were usually more negative than −40 mV, but neurons with membrane potentials between −30 and −40 mV were not excluded from analysis of fiber types, because deterioration of the membrane potential did not affect the latency of the evoked action potential. Recordings often lasted for only a few minutes, so no further electrophysiological measurements were performed. After determining the latency and threshold, the neuron was filled with LY by passing hyperpolarizing current through the electrode. The filling of the neuron was followed under fluorescent light and stopped at a certain degree of filling (quantified as fluorescence intensity detected by the CCD camera at a defined exposure time at 428-mn excitation wavelength) that later would help with reidentification of the neuron. The electrode was then withdrawn and the cross-sectional area of the neuron measured. After each filling of a neuron or unsuccessful attempt at penetration, the surroundings of the filled or targeted neuron were checked under epifluorescence to exclude accidental, undesired filling of neighboring or uncharacterized neurons.

Two to six neurons were recorded and filled in one ganglion in this way. Care was taken to choose neurons lying clearly apart in the longitudinal (dorsal root-spinal nerve) axis. The position of each filled neuron in the ganglion with respect to the dorsal root/spinal nerve and the other filled neurons was noted and photographically documented along with its size, shape, and degree of filling with LY. The degree of filling was again verified immediately before fixation of the ganglion to ensure that no leakage of the dye had occurred. At the end of the recordings, the DRG was carefully removed from the recording chamber and fixed by immersion in 4% PFA in 0.1 M phosphate buffer (PB) for 18 hours at 4°C.

The corrected conduction velocity of the fiber of a recorded DRG neuron was determined from the action potential latency (onset of the stimulation to onset of the action potential recorded in the DRG cell soma) and the length of the stimulated nerve segment (measured from stimulation cathode to the centre of the DRG), corrected, where applicable, by the utilization time as described in Results. The length of the stimulated nerve segment was 3–6 mm for the L4 ganglion (connected to the L4 spinal nerve) and 12–20 mm for the L5 ganglion (in continuity with the L5 spinal nerve and sciatic nerve).

Immunohistochemistry

Tissue processing and staining procedures. After fixation (see above) and cryoprotection (20% sucrose in PB for 48 hours at 4°C), DRGs were snap frozen and stored at −80°C. Starting at the spinal nerve entry zone, the entire DRG was cut into 5-μm sections on a cryostat (CM 3050; Leica, Nussloch, Germany), mounted on SuperFrost Plus slides (Menzel, Braunschweig, Germany), and air dried. LY-filled cells were visualized under a fluorescence microscope (B51; Olympus, Tokyo, Japan) and identified according to their location with respect to the dorsal root/spinal nerve and the other filled neurons and their shape, size, and degree of filling. These parameters allowed unequivocal reidentification of most (>85%) filled neurons in the cryosections. Neurons that could not be identified with certainty were excluded from analysis. For reidentified neurons, two adjacent sections containing the nucleus of the filled neuron were stained with the following sets of antibodies. Set 1 consisted of biotin-conjugated IB4 (1:200), rat anti-SP (1:2,000), and rabbit anti-NPY (1:2,000). Set 2 comprised mouse anti-NF200 (1:4,000), sheep anti-CGRP (1:1,000), and fluorescein isothiocyanate (FITC)-conjugated IB4 (1:200). The secondary reaction, where applicable, was conducted with streptavidin-conjugated AMCA (1:200), Cy3-conjugated donkey anti-rat IgG (1:400), Cy5-conjugated donkey anti-rabbit IgG (1:200), AMCA-conjugated donkey anti-mouse IgG (1:200), and Cy3-conjugated donkey anti-sheep IgG (1:400). IB4 was included in both sets for control and gave identical results. Randomly selected sections of the same DRGs not contain-

The Journal of Comparative Neurology. DOI 10.1002/cne

328

R. RUSCHEWEYH ET AL.

ing LY-filled neurons were processed in the same way with either of the two antibody sets to obtain results from larger samples of neurons that were then, however, unidentified with respect to their fiber type.

Primary antibodies and biotin-conjugated IB4 were diluted in 0.1 M phosphate-buffered saline (PBS) containing 0.3% Triton X-100 and 5% normal donkey serum and incubated overnight at 4°C. Secondary antibodies and FITC-conjugated IB4 were diluted in 0.1 M PBS and incubated for 3 hours at room temperature. Sections were washed with 0.1 M PBS between steps and before coverslipping them in a glycerine-based antifading medium, containing Mowiol (Hoechst, Frankfurt, Germany) and propyl gallate (Sigma-Aldrich, St. Louis, MO). Controls made by omission of one of the primary or secondary antibodies to check for bleed-through, cross-reactions, and nonspecific reactions were always negative for the chosen combinations of antibodies.

Antibodies and binding agents. Rat anti-SP [BD PharMingen, San Jose, CA; No. 556312; lot No. 42669, monoclonal, clone NC1/34, immunizing antigen: SP conjugated to bovine serum albumin (BSA)] recognizes an epitope in the carboxy-terminal region of SP and shows no cross-reactivity with other brain peptides, including [Leu]enkephalin, [Met]enkephalin, somatostatin, and β-endorphin (Cuello et al., 1979). A polyclonal anti-SP antibody [DiaSorin, Stillwater, MN; No. 20064, lot No. 313003, raised in rabbit against SP coupled to a carbodiimide/keyhole limpet hemocyanin (KLH) conjugate], yielded identical results in DRGs and spinal cord. Sheep anti-CGRP was from Biomol (Plymouth, PA; No. CA1137, lot No. Z05180, polyclonal, raised against whole-rat α-CGRP conjugated to BSA). Preincubation of 1 ml of the diluted antiserum with rat 10 nmol α-CGRP but not with galanin or SP abolished the immunostaining in rat spinal cord (manufacturer's information). Staining in mouse DRGs and spinal cord was the same as with a rabbit anti-CGRP (Biomol; No. CA1134, lot No. Z05177, polyclonal, raised against the same immunogen) and matched the distribution of mRNA and protein reported in the literature (Fukuoka et al., 1998; Tie-Jun et al., 2001). Mouse anti-NF200 (Sigma-Aldrich; No. N0142, lot No. 124K4778, monoclonal, clone N52, raised against the C-terminal segment of enzymatically dephosphorylated pig neurofilament H-subunit) is specific for 200-kD neurofilament (=NF-H; phosphorylated and nonphosphorylated) in rat spinal cord extract on immunoblot. The antibody does not cross-react with the other intermediate filament proteins (manufacturer's information) and has been well established as a marker of presumably myelinated DRG neurons (Lawson and Waddell, 1991; Hammond et al., 2004). Rabbit anti-NPY (Sigma-Aldrich; No. N9528, lot No. 101K4881, polyclonal, raised against synthetic NPY conjugated to KLH) antiserum has been tested by radioimmunoassay for cross-reactivity with PYY, vasoactive intestinal peptide (VIP), somatostatin, insulin, and other peptides and shown to be specific for NPY (manufacturer's certificate of analysis). In our hands, this antibody showed the typical NPY staining patterns in spinal cord and DRGs and reaction of these patterns to peripheral nerve injury that have been previously described in rat (Shehab et al., 2003; Brumovsky et al., 2004) and mouse (Corness et al., 1996). Biotin- and FITC-conjugated IB4 was from Vector Laboratories (Burlingame, CA; No. B-1205 and FL-1201). The secondary antibodies used here were produced in donkey and are affinity purified and especially qualified for multiple labelling (Jackson Immunoresearch, West Grove, PA).

Immunohistochemical data acquisition and analysis. Sections were examined under the fluorescence microscope with the appropriate filter sets. Fluorescence images were acquired with a CCD camera (Olympus DP50), and AnalySIS software (Soft Imaging Systems, Münster, Germany) was used for image acquisition and measurements. LY-filled neurons were evaluated with respect to their expression of the five markers included in the two staining sets described above.

Staining and size distribution of unidentified DRG neurons were evaluated in three to five pairs of sections (i.e., adjacent sections stained with antibody sets 1 and 2, respectively). Pairs of sections were randomly chosen but never closer than 60 μm to the next pair of sections. Two hundred fifty to three hundred fifty cells were analyzed per set and animal. Digital images of the chosen sections were acquired with a ×20 objective, and all neurons with a visible nucleus were evaluated with respect to their cross-sectional area and to the presence or absence of the five markers. For a given staining, exposure time, contrast, and resolution were kept constant throughout sections and animals, and the fluorescence intensity of each cell was evaluated on a subjective scale from 0 to 3 (0 = no staining, 1 = weak staining, 2 = strong staining, 3 = very strong staining). Neurons reaching a rating of 1 or higher were considered positive for the respective marker. Similarly to the usual procedure in the rat (see, e.g., Noguchi et al., 1994; Hammond et al., 2004), neurons were divided into three size groups (small, <300 μm^2; medium-sized, $300-700$ μm^2; large, >700 μm^2). Data from L4 and L5 DRGs were pooled throughout the study.

Note that the cross-sectional areas reported for the electrophysiologically identified neurons (e.g., Table 1) were measured in living tissue and therefore cannot directly be compared with the values measured after processing for immunohistochemistry (e.g., Fig. 5, Table 2). Cell areas were estimated to shrink to 89% ± 4% during this procedure (from 18 neurons in which areas were evaluated both in the living tissue and after immunohistochemistry).

AnalySIS software was used for image acquisition, storage, and manipulation. For better reproduction, brightness and contrast of the immunohistochemical images shown in Figures 2 and 3 were enhanced, and, for AMCA stainings, the hue of the blue channel was slightly reduced. Corel Draw 9 (Corel Corporation, Ontario, Canada) was used for final figure layout.

Statistical analysis

All data are given as mean ± SEM. Statistical significance was assessed by a Mann-Whitney rank sum test or Fisher's exact test followed by Bonferroni correction or by a two-way ANOVA followed by a Tukey test as indicated in the text.

RESULTS
Behavior

As described previously for the same strain (Schoffnegger et al., 2006), mice developed significant mechanical allodynia and thermal hyperalgesia in the ipsilateral hindpaw on the day following loose ligation of the sciatic

The Journal of Comparative Neurology. DOI 10.1002/cne

PRIMARY AFFERENT MARKERS AFTER NERVE INJURY

329

nerve, and this behavior remained stable throughout the examination period (mechanical thresholds preoperatively: 0.93 ± 0.12 g, on day 1 after ligation: 0.09 ± 0.03 g, on day 9 after ligation: 0.01 ± 0.00 g; thermal withdrawal latencies at the same time points: 6.1 ± 0.2 seconds, 1.8 ± 0.1 seconds, and 1.3 ± 0.1 seconds; n = 7, $P < 0.01$, two-way ANOVA followed by Tukey test). No allodynia or hyperalgesia was seen in the contralateral paws of CCI mice or in the ipsi- or contralateral paws of sham-operated mice (n = 5–7, $P > 0.05$ in the respective Tukey tests).

Conduction velocity limits among Aβ-, Aδ-, and C-fibers

To determine the conduction velocity borders between different fiber types under our experimental conditions (7–12-week-old mice, 22–24°C), we recorded compound

action potentials (CAPs) from sciatic nerves of naïve and neuropathic mice. Aβ-, Aδ-, and C-fiber components of the CAP could be distinguished according to their conduction velocities in response to electrical stimulation of the sciatic nerve (Fig. 1A,B). Aδ- and C-fiber CAPs were clearly separated at a conduction velocity of 1 m/second, independently of the distance between stimulating and recording electrode. However, CAPs of Aβ- and Aδ-fibers often lay closely together, and the conduction velocity border between Aβ- and Aδ-fibers proved to be strongly dependent on the distance between electrodes (Fig. 1C). This presumably was due to the utilization time (the delay between the electrical stimulus and the generation of an action potential in the stimulated fiber; Djouhri and Lawson, 2001), an artefact that has a larger impact on conduction velocities calculated from short than from long nerve segments. There was no obvious difference between naïve and neuropathic nerves, so the data were pooled and fitted by a curve following the utilization time equation (Fig. 1C). The fit resulted in a utilization time of 0.9 msec and a real conduction velocity border between Aβ- and Aδ-fibers of 13 m/second. Therefore, latencies measured from single nerve fibers (see below) conducting in the Aβ- or Aδ-fiber range were corrected for the utilization time, and conduction velocities calculated from the corrected latencies were judged to fall into the Aδ-fiber range (1–13 m/second) or the Aβ-fiber range (>13 m/second). Fibers conducting at <1 m/second were classified as C-fibers.

Classification of DRG neurons as Aβ-, Aδ-, or C-fiber neurons

In total, 127 neurons (74 in naïve and sham operated mice, 53 in neuropathic mice) were recorded and filled with LY (Fig. 1D,E) and later successfully reidentified for immunohistochemistry (see below). They were classified as neurons with Aβ-, Aδ-, and C-fibers according to their conduction velocities (Fig. 1F) as described
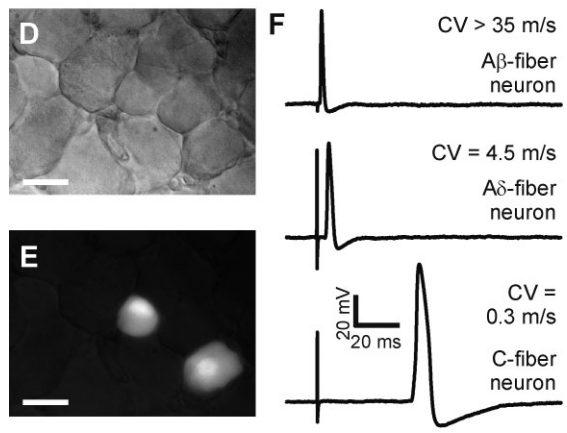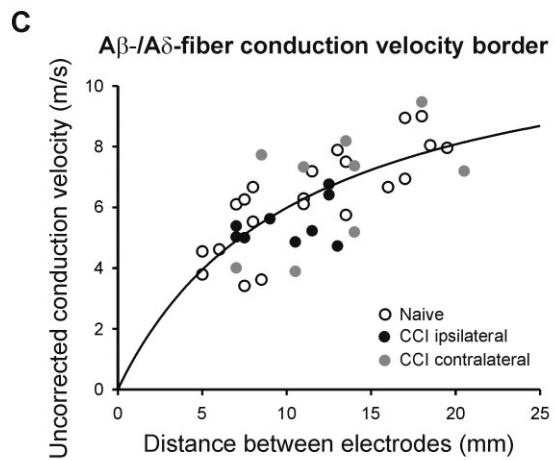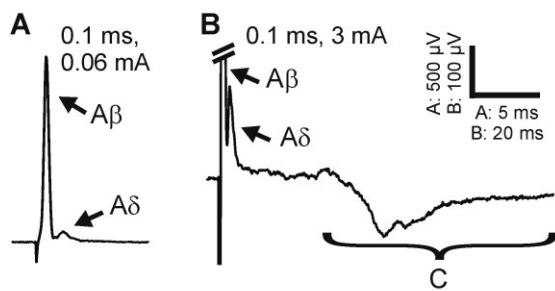
Fig. 1. Electrophysiological identification of DRG neurons as Aβ-, Aδ-, or C-fiber neurons. A–C: Conduction velocities in the sciatic nerve of the mouse. A,B: Examples of sciatic nerve compound action potentials (CAPs) in response to single-shock electrical stimulation of the nerve. **A:** At low stimulation intensity, Aβ- and Aδ-fiber CAPs were evoked. **B:** At high stimulation intensity, the stimulus artefact distorted the Aβ-fiber CAP, and a C-fiber CAP became visible. Curves are averaged from six consecutive responses to stimulation. Distance between stimulating and recording electrode was 18.5 mm. **C:** The uncorrected conduction velocity limit between Aβ- and Aδ-fibers, as calculated by (distance between electrodes)/(latency of the CAP), was dependent on the distance between electrodes, presumably because of the time needed by an electrical stimulus to evoke an action potential (utilization time). The data points were fitted by the utilization time equation $y = x \cdot CV/(x + CV \cdot UT)$, to find the utilization time (UT) and the real conduction velocity border (CV) between Aβ- and Aδ-fibers. Ipsilateral nerves from neuropathic animals had a maximum length of 15 mm, because the portion of the nerve covered by the ligatures was resected. D–F: Recording of DRG neurons. **D:** Transmission image of the surface of a DRG from a neuropathic animal. DRG neurons of various sizes can be distinguished. **E:** Fluorescence image of the same section taken at 427 nm illumination. Two neurons have been recorded and filled with lucifer yellow (LY). The smaller neuron conducted at C-fiber velocity, the larger at Aδ-fiber velocity. **F:** Examples of the responses of three neurons belonging to the three fiber groups to stimulation of the sciatic nerve. Distance between electrodes was 12.5 mm. CV, conduction velocity corrected for utilization time (see Results). Scale bars = 20 μm.

The Journal of Comparative Neurology. DOI 10.1002/cne

330   R. RUSCHEWEYH ET AL.

TABLE 1. Properties of the Recorded DRG Neurons[1]

		Aβ-fiber neurons	Aδ-fiber neurons	C-fiber neurons
Conduction velocity (m/second)	Control	[23.9 ± 2.5 (13)]	5.6 ± 0.7 (23)	0.3 ± 0.0 (38)
	Neuropathic	[31.0 ± 1.6 (20)]	6.8 ± 0.8 (15)	0.3 ± 0.0 (18)
Stimulation threshold at 0.1-msec	Control	0.44 ± 0.17 (13)	0.62 ± 0.16 (20)	1.74 ± 0.27 (38)
pulse width (mA)	Neuropathic	0.49 ± 0.11 (16)	0.63 ± 0.20 (13)	1.72 ± 0.38 (16)
Cross-sectional area (μm^2)	Control	1,171 ± 72 (12)	943 ± 62 (23)	418 ± 18 (38)
	Neuropathic	1,086 ± 83 (20)	776 ± 37 (15)	455 ± 30 (18)

[1]Numbers of neurons are given in parentheses. Differences between control and neuropathic neurons were not significant (two-way ANOVA). In some experiments, only the short (3-6 mm) spinal nerve was available for stimulation (see Materials and Methods). The fastest-conducting Aβ-fibers sometimes produced very short latencies to stimulation in these short nerve segments that after correction for utilization time resulted in unrealistically high conduction velocities. We judged this to be due to the limited precision of latency measurement that produces proportionally larger errors in short than in long latencies. It was estimated that a conduction velocity of 35 m/second was the maximum that could be accurately determined in these short nerves, and fibers that apparently conducted more rapidly were assigned this conduction velocity. The mean conduction velocity of Aβ-fibers given here in brackets is therefore probably lower than the real value. This problem inherently affects latency measurements of the fastest-conducting fibers (in the upper Aβ-fiber range) much more than slower-conducting fibers (near the Aβ-/Aδ-fiber conduction velocity border), so it is not likely to have compromised DRG neuron classification.
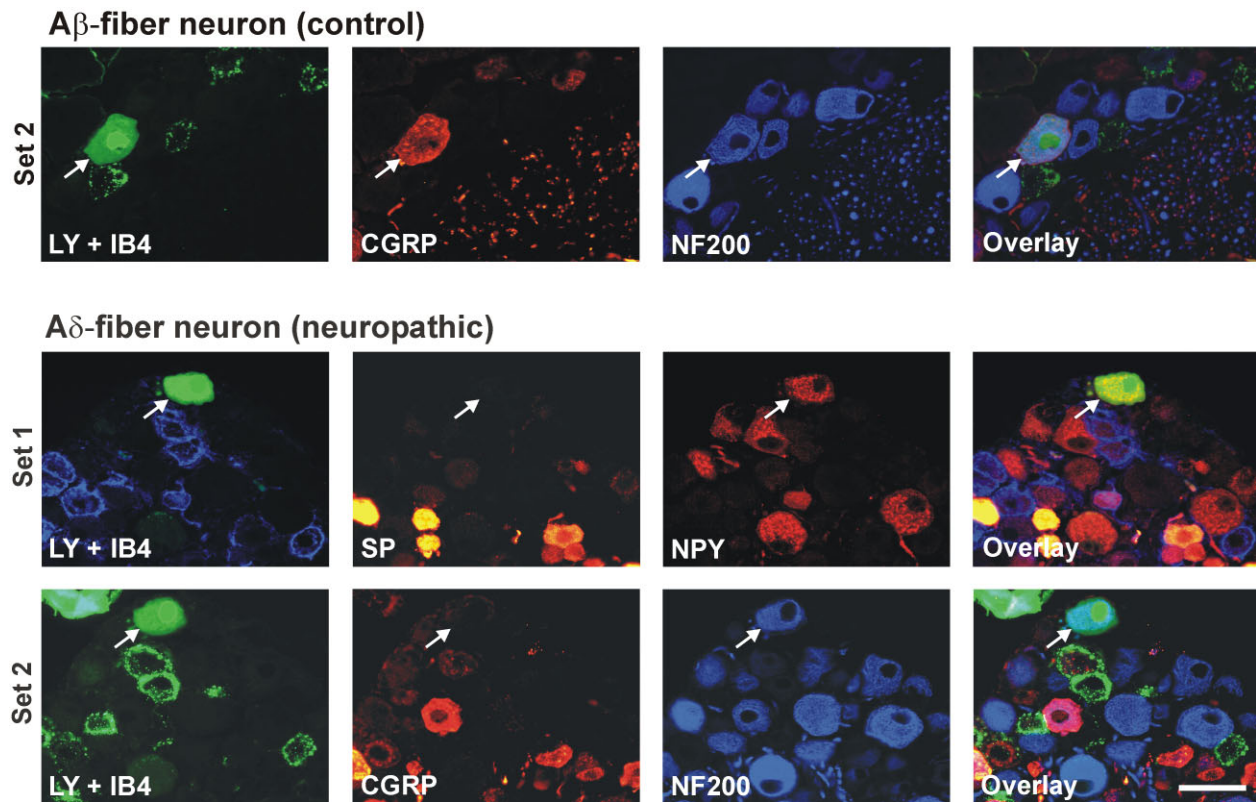
Fig. 2. Examples of typical neurochemical patterns in neurons with A-fibers. An A-fiber neuron from a control animal expressed calcitonin gene-related peptide (CGRP) and neurofilament 200 (NF200) whereas one from a neuropathic animal expressed NF200 and neuropeptide Y (NPY) but no CGRP. Staining sets are as defined in Materials and Methods. IB4, isolectin B4; SP, substance P. Scale bar = 50 μm.

above. Conduction velocities, stimulation thresholds, and sizes of the different cell types are shown in Table 1. Even if the mean cross-sectional cell areas increased from C- over Aδ- to Aβ-fiber neurons, area ranges largely overlapped (C: 178–687 μm^2, Aδ: 527–1,588 μm^2, Aβ: 558–1,993 μm^2), showing that classification of DRG cells as Aβ-, Aδ-, or C-fiber neurons according to cell size is imprecise.

Neurochemical patterns in identified Aβ-, Aδ-, and C-fiber neurons

A-fiber neurons. Aβ- and Aδ-fiber neurons showed similar patterns, albeit with different incidence. Virtually all neurons with A-fibers in control animals expressed NF200 and 30–40% additionally were immunoreactive for CGRP. In neuropathic animals, many neurons with A-fibers additionally expressed NPY, especially those that were not immunoreactive for CGRP (Fig. 2).

C-fiber neurons. In control animals, neurons with C-fibers either bound IB4 (47%) or expressed CGRP and/or SP (47%). Only 3% expressed none of the tested markers. In neuropathic animals, the peptidergic group was smaller, and about 23% expressed none of the markers (Fig. 3).

Figure 4A–C shows the overall expression of the tested markers for the three groups of neurons. The most prom-
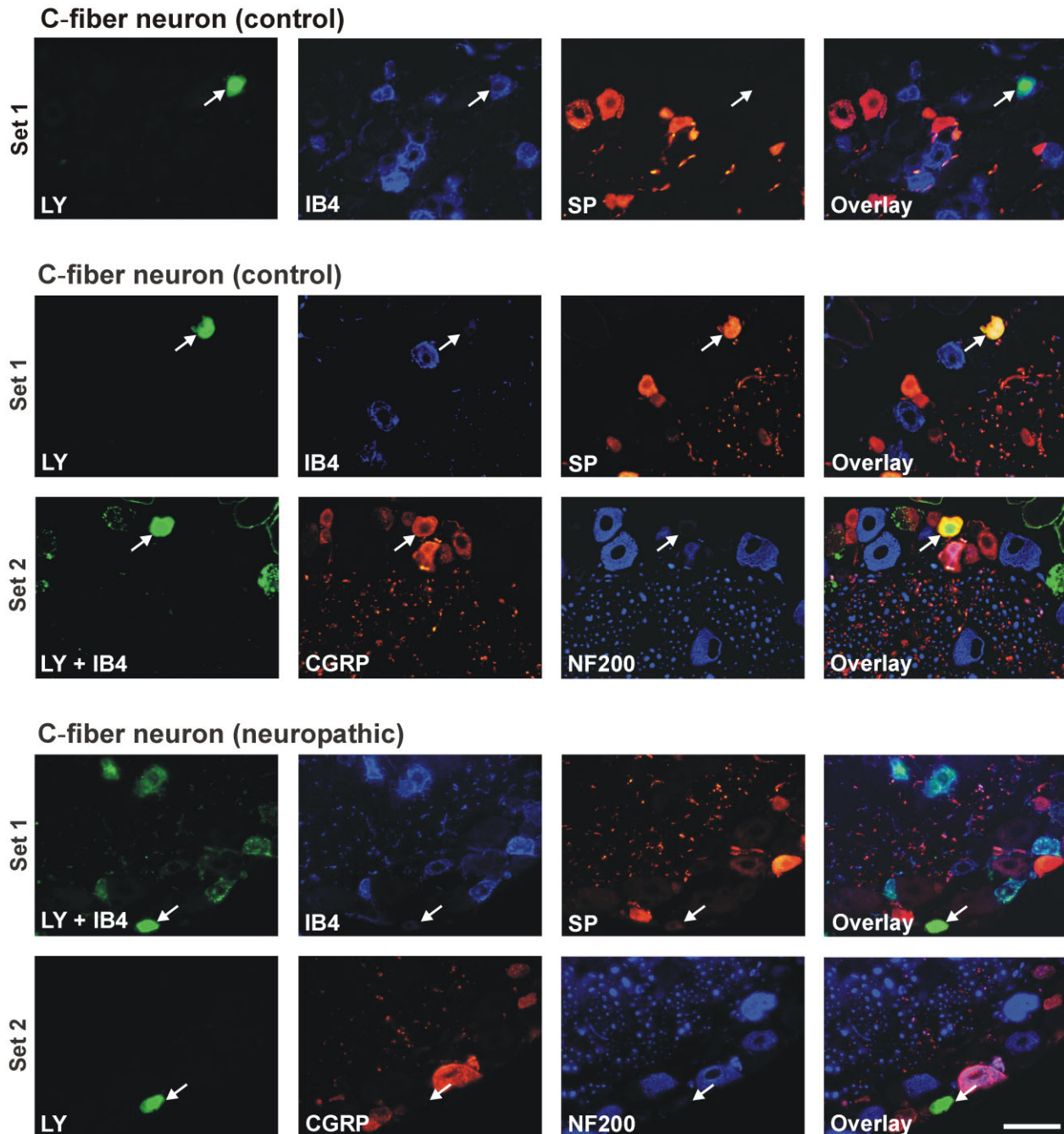
Fig. 3. Examples of typical neurochemical patterns in neurons with C-fibers. C-fiber neurons from control animals illustrate a neuron that expresses IB4 but no SP and a neuron that expresses SP and CGRP but no IB4. The C-fiber neuron from the neuropathic animal is an example of a neuron that expresses none of the tested markers. NPY is not shown but was negative in all three cells. Staining sets correspond to those defined in Materials and Methods except for the C-fiber neuron from the neuropathic animal, where FITC-coupled IB4 was included in set 1 instead of set 2. Scale bar = 50 μm.

inent difference was the de novo expression of NPY in neurons with A-fibers in the neuropathic animal. There was a trend toward reduction in the number of C-fiber neurons expressing SP and CGRP, but much larger cell numbers would have been needed to reach significance.

For practical purposes, it is useful to know the "positive predictive value" of a given marker for a certain group, i.e.,

the probability that a DRG neuron expressing the marker is an A- or C-fiber neuron. To calculate predictive values, it is necessary to know the relative incidence of A- and C-fiber neurons in the DRG, which has been estimated to be about 30%/70% (A-/C-fiber neurons) in the normal animal based on counts of myelinated and unmyelinated fibers in the dorsal roots or large light and small dark cells in the DRG (Cogge-

The Journal of Comparative Neurology. DOI 10.1002/cne

332   R. RUSCHEWEYH ET AL.

shall et al., 1997; Tandrup et al., 2000). For these conditions, we calculated the following predictive values: IB4, C-fiber, control 100%, neuropathic 100%; SP, C-fiber, control 92%, neuropathic 84%; CGRP, C-fiber, control 73%, neuropathic

59%; NF200, A-fiber, control 89%, neuropathic 86%, NPY, A-fiber, neuropathic: 82%. Thus, for example, if one observes an SP-immunoreactive neuron in a control animal, the probability that it is a C-fiber neuron is 92%. The predictive values of a given marker for A- and C-fiber neurons sum up to 100%, but only the higher of the two values has been given. Of course, because of the limited number of neurons investigated and because the exact relation of A- to C-fiber neurons is not known, these predictive values are only approximations.

Neurochemical markers in unidentified DRG neurons

To compare the results from our identified neurons with a larger neuronal sample and to assess the size distribution of the markers, we performed immunohistochemistry on DRG neurons unidentified with respect to their fiber type (250–350 neurons evaluated per marker and animal). The incidence of the tested markers and their modification after nerve injury were consistent with the results in identified neurons (Fig. 4D). The overall size distribution of unidentified DRG neurons (Fig. 5A) showed a nonsignificant trend toward a size shift from small to medium-sized cells in neuropathic animals ($P > 0.05$, Mann-Whitney test followed by Bonferroni correction). The distribution of neurochemical markers in control and neuropathic animals among DRG neurons of different sizes is shown in Figure 5 and Table 2. In neuropathic animals, IB4, SP, and CGRP were preferentially reduced in small neurons. A small increase was seen in SP-immunoreactive medium-sized neurons after CCI. NPY was up-regulated in medium-sized and large neurons.

To corroborate the finding that up-regulation of NPY in the neuropathic animal takes place in those neurons with A-fibers that do not express CGRP, a triple staining for NF200, CGRP, and NPY was performed in unidentified DRG neurons. After nerve injury, $17\% \pm 3\%$ of the NF200-immunoreactive neurons expressed CGRP, and $33\% \pm 5\%$ expressed NPY, but only $1\% \pm 0\%$ were immunoreactive for both markers (n = 3 mice, 250–350 NF200-immunoreactive neurons counted per animal).

Correlation between neurochemical markers and behavior

It has been discussed that changes of neurochemical markers after nerve injury may represent an adaptive phenomenon, e.g., by counteracting the expression of neuropathic pain. If this were the case, then more adaptation should result in less pain. We therefore correlated the pain behavior of neuropathic animals on days 7 and 9 after the operation (corresponding to the last two measurements before death) to the expression of neurochemical markers. This
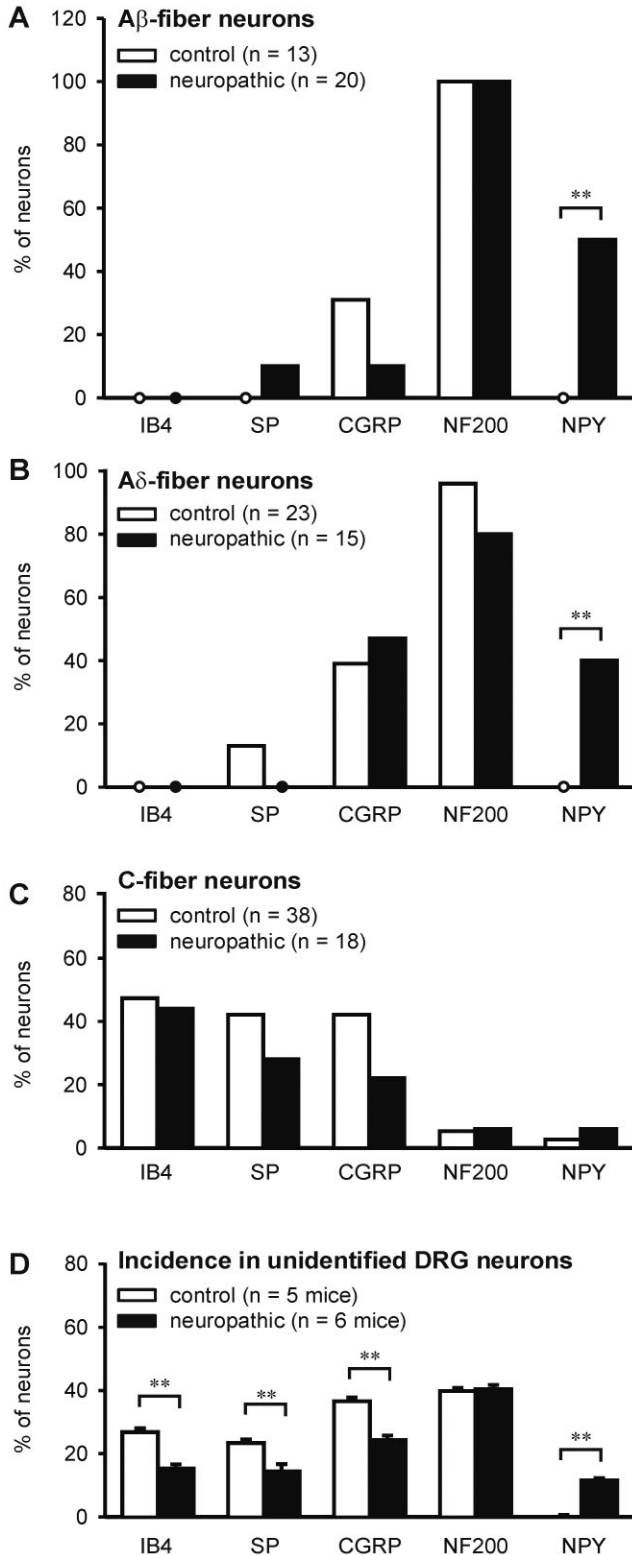
Fig. 4. Distribution of neurochemical markers in DRGs from control and neuropathic mice. **A–C:** Distribution of markers in electrophysiologically identified Aβ-, Aδ-, and C-fiber neurons. For each marker, the percentage of neurons positive for this marker in the corresponding fiber group is illustrated. Circles on the baseline indicate no expression of the respective marker. **P < 0.01 on Fisher's exact test followed by Bonferroni correction. **D:** Distribution of markers in a larger sample of electrophysiologically unidentified L4 and L5 DRG neurons; 250–350 neurons were counted per marker and animal. **P < 0.01 (Tukey test following two-way ANOVA).
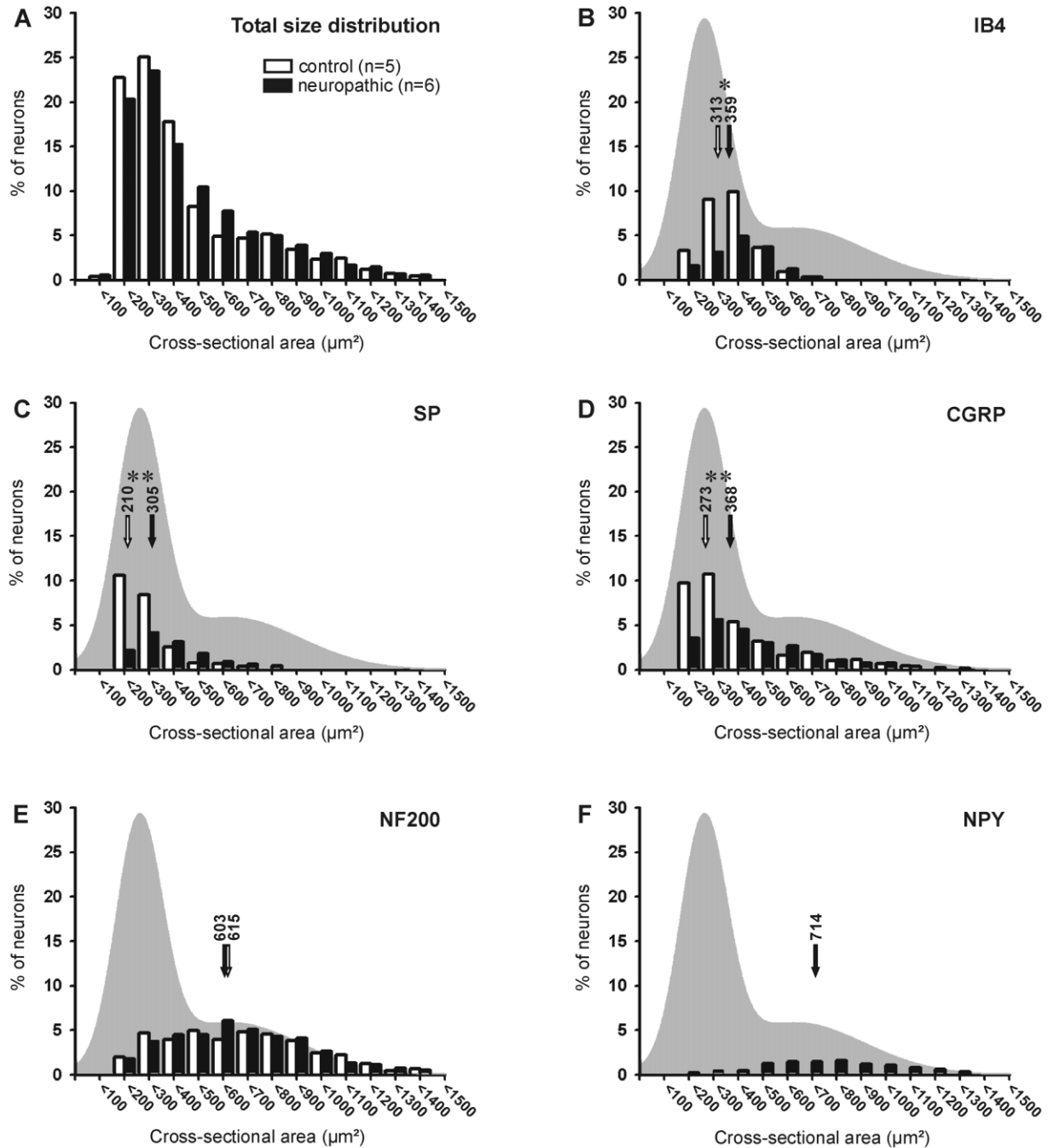
Fig. 5. Size distribution of neurochemical markers in DRGs from control and neuropathic mice. **A:** Overall size distribution of DRG neurons in control and neuropathic mice. **B–F:** Size distributions of DRG neurons that bound IB4 or were SP, CGRP, NF200, and NPY immunoreactive. Percentages are relative to the total DRG population. The gray area illustrates the overall size distribution in control animals, calculated by fitting the distribution by the sum of two normal distributions. Arrows represent median cell sizes of the groups. The size distributions of IB4, SP, and CGRP were significantly shifted to larger cells in neuropathic animals, reflecting a preferential loss of small DRG neurons staining for the respective marker. *$P < 0.05$, **$P < 0.01$ (on Tukey test following two-way ANOVA); n, number of animals.

was possible only for the paw withdrawal latencies in response to heat, insofar as the von Frey thresholds of all neuropathic animals were virtually identical at the bottom of the scale. No correlation was seen for IB4, SP, CGRP, or NF200, but we found a strong correlation between paw with-drawal threshold and NPY expression (Fig. 6; Spearman correlation coefficient 0.98, $P < 0.01$; note that the paw withdrawal latency decreases with increasing pain sensitivity so that there is an *inverse* relationship between NPY expression and the degree of thermal hyperalgesia).

The Journal of Comparative Neurology. DOI 10.1002/cne

334

R. RUSCHEWEYH ET AL.

TABLE 2. Distribution of the Neurochemical Markers Among Cells of Different Sizes in DRGs From Control and Neuropathic (CCI) Animals[1]

	Small cells (<300 μm²)		Medium-sized cells (300-700 μm²)		Large cells (>700 μm²)	
	Control (n = 5)	CCI (n = 6)	Control (n = 5)	CCI (n = 6)	Control (n = 5)	CCI (n = 6)
IB4	12 ± 1(25 ± 2)	5 ± 0[3](11 ± 1)	15 ± 1(41 ± 3)	10 ± 1[3](26 ± 1)	0 ± 0(1 ± 0)	0 ± 1 (1 ± 0)
SP	19 ± 1(39 ± 2)	7 ± 1[3](16 ± 2)	4 ± 1(12 ± 2)	7 ± 1[2](18 ± 2)	0 ± 0(2 ± 1)	1 ± 0 (5 ± 2)
CGRP	20 ± 2(41 ± 3)	9 ± 1[3](21 ± 2)	12 ± 1(33 ± 4)	12 ± 1 (3 ± 3)	4 ± 0(22 ± 2)	3 ± 0 (21 ± 2)
NF200	6 ± 1(13 ± 2)	6 ± 1 (13 ± 2)	18 ± 2(50 ± 4)	20 ± 1 (51 ± 2)	16 ± 2(100 ± 9)	15 ± 1 (93 ± 4)
NPY	0 ± 0(0 ± 0)	1 ± 0 (2 ± 1)	0 ± 0(0 ± 0)	5 ± 1[3](13 ± 2)	0 ± 0(1 ± 1)	7 ± 1[3](42 ± 7)

[1]Numbers are percentages of neurons expressing the respective marker in relation to the total cell population. Numbers in parentheses are percentages of neurons expressing the respective marker in relation to the population of cells in the respective size group. Between 250 and 350 neurons were analyzed per marker and animal. Please note that comparisons of cell numbers between size groups are necessarily inaccurate, because we used profile counting methods that are known to overestimate large cells. n, Number of animals. For each size group, a two-way ANOVA followed by a Tukey test was used to detect significant differences between control and CCI animals.
[2]$P < 0.05$ on Tukey test.
[3]$P < 0.01$ on Tukey test.
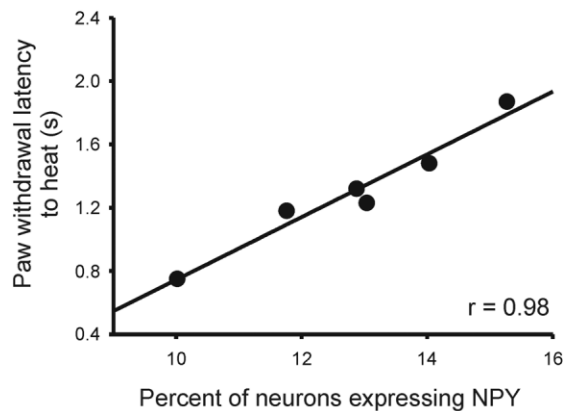
Fig. 6. Correlation between behavior and NPY expression in neuropathic animals. For six neuropathic mice, the percentage of NPY-immunoreactive neurons in L4 and L5 DRGs was evaluated and correlated with the average of the paw withdrawal thresholds to heat measured on days 7 and 9 after induction of the neuropathy.

DISCUSSION

The main goal of the present study was to determine whether the classical neurochemical markers of primary afferent neurons with A- and C-fibers remain valid in neuropathic pain resulting from a peripheral nerve lesion. Ten days after CCI of the sciatic nerve, NF200 and IB4 remained markers for A- and C-fiber neurons, respectively. The predictive value of SP for C-fiber neurons decreased somewhat after nerve injury but was still above 80%. Both IB4 and SP/CGRP were down-regulated, resulting in a considerable number of C-fiber neurons (~20%) that expressed none of the tested markers after nerve injury, so care must be taken not to exclude these neurons unintentionally from study when identification of fiber types is based on these markers. NPY is up-regulated in A-fiber neurons after nerve injury.

Choice of the neuropathic model

It is well known that not only injured but also neighboring, healthy DRG neurons are affected by nerve injury, sometimes in opposite directions (Ma and Bisby, 1998b,c). For example, SP seems to be lost in axotomized neurons but up-regulated in neighboring, uninjured neurons in the rat (Ma and Bisby, 1998a). Both of these mechanisms can possibly lead to disruption of the specificity of the neurochemical markers for A- or C-fiber neurons, so we chose a model in which axotomized and uninjured neurons coexist in the same nerve, the CCI (loose ligation of the sciatic nerve). Electrical stimulation was applied proximal to the nerve ligatures to include both injured and uninjured neurons in the studied population. Injured and uninjured neurons are two separate groups, so de novo expression of a C-fiber neuron marker in A-fiber neurons in, e.g., injured neurons, cannot be obscured by processes in the uninjured group. The CCI model is also a clinically relevant model, because most clinical nerve injuries are partial.

Use of corrected conduction velocities for the classification of DRG neurons according to their fiber types

As explained in Materials and Methods, the nerve segment available for measuring the conduction velocity was different in L4 ganglia (3–6 mm) vs. L5 ganglia (12–20 mm). Disregarding the utilization time introduces a substantial error in the calculation of conduction velocities, which is larger in short than in long nerve segments (Fig. 1C; Djouhri and Lawson, 2001). Taking into account the utilization time and calculating corrected conduction velocities enabled us to classify correctly fibers whose conduction latencies were measured in nerves of differing lengths.

The utilization time resulting from the present data (0.9 msec) is somewhat longer than that previously described (0.3–0.7 msec for Aβ- and Aδ-fibers in the guinea pig; Djouhri and Lawson, 2001), possibly because of the lower recording temperature or the characteristics of the stimulation electrode used in the present study. The corrected Aβ-/Aδ-fiber conduction velocity border (13 m/second) is similar to previous uncorrected values measured in long nerves, where the error introduced by the utilization time is small (mouse: 10 m/second; rat: between 8 and 27 m/second, Koltzenburg et al., 1997; Baba et al., 1999). Many groups use short nerve segments that, when not corrected, yield much lower Aβ-/Aδ-fiber conduction velocity borders (e.g., 4.2 m/second in guinea pig nerves of 4–6 mm length and 6.5 m/second in rat nerves of 7.7 mm length, compare with Fig. 1C; Djouhri and Lawson, 2001; Fang et al., 2006).

Comparison between identified and unidentified DRG neurons

Qualitatively similar changes of markers were observed in the electrophysiologically identified neurons and the larger sample of unidentified DRG neurons. No quantitative comparison was attempted because of several differ-

The Journal of Comparative Neurology. DOI 10.1002/cne

PRIMARY AFFERENT MARKERS AFTER NERVE INJURY

335

ences in the studied populations. To maximize the impact of the nerve lesion on our identified neurons, we recorded only neurons with an axon in the sciatic nerve, but about 20% of mouse L5 DRG neurons have their axon elsewhere (Shi et al., 2001). Whereas almost every targeted neuron could be impaled, recorded, and stained in the control DRGs, small neurons in neuropathic DRGs were often fragile, and not every recording was successful. If injured neurons were frailer than neighboring, healthy neurons then this may be an explanation for the surprisingly small decrease in IB4-binding neurons in identified compared with unidentified neurons. Finally, we did not use stereological methods for the overall cell counts, and this is known to lead to an overestimation of the proportion of large DRG neurons (Shi et al., 2001).

Size distribution of the neurochemical markers

We found a significant reduction of small IB4-binding and SP- and CGRP-immunoreactive DRG neurons after CCI. Consistently, about 20% of the electrophysiologically identified C-fiber neurons did not express any of these markers after CCI. In addition, the overall cell size distribution was comparable in DRGs from control and neuropathic animals. This suggests that the loss of staining for IB4, SP, and CGRP was due not to cell death but rather to a decreased expression of the respective antigens.

Different neuropathic models seem to cause different shifts in the size distribution of the neurochemical markers tested here. Whereas in the CCI model in mice and rats (present study; Schäfers et al., 2003) the reduction of IB4-binding neurons was most marked among small DRG cells, a loss of IB4-binding neurons without size preference was seen in the L5 DRG after L5/L6 tight spinal nerve ligation in the rat (Hammond et al., 2004). Similarly, we found that the reduction of CGRP-immunoreactive neurons was exclusively located in the small cell fraction, whereas after spinal nerve ligation loss of CGRP immunoreactivity was predominant in large cells (Hammond et al., 2004). Although no size shift in neurons staining for NF200 was observed in the present study, Hammond et al. (2004) reported a loss of large NF200-immunoreactive neurons and a compensatory increase of small and medium-sized neurons that expressed NF200 after spinal nerve ligation. In contrast, independently of the model, NPY expression is induced preferentially in medium-sized and large DRG neurons after nerve injury in mice and rats (present study; Wakisaka et al., 1992; Shi et al., 1999). After a tight spinal nerve ligation, most or all neurons of the respective ganglion are axotomized, but CCI produces an intermingling of axotomized and healthy fibers, which are sometimes affected in opposing directions (Ma and Bisby, 1998b,c). This might be a reason for the differences in size distribution shifts between the two models.

Evidence for expression of SP in Aβ-fibers after nerve injury

In normal animals, SP is a nociceptive transmitter and, among the primary afferents, is expressed mainly by C-fiber neurons (Lawson et al., 1997, 2002: guinea pig). It has been proposed that, after peripheral inflammation or nerve injury, nonnociceptive Aβ-fibers start to express SP and release it in the spinal dorsal horn. This would be a tempting explanation for allodynia (pain evoked by nonnoxious stimuli, a typical symptom of neuropathic pain after peripheral nerve injury; Woolf, 2004; Zieglgäns-

berger et al., 2005). The histochemical evidence for the occurrence of this phenomenon after nerve injury in the rat is only partially favorable (Noguchi et al., 1994, 1995; Marchand et al., 1994; Ma and Bisby, 1998a; Allen et al., 1999).

In the present study, after CCI of the sciatic nerve, two of 20 Aβ-fiber neurons expressed SP as opposed to zero of 13 in the control animals. This difference was not significant at the number of neurons investigated. The two SP-expressing Aβ-fiber neurons had high conduction velocities (>35 m/second) and low stimulation thresholds (0.03 and 0.06 mA), making it unlikely that they were misclassified Aδ-fiber neurons. However, they were among the smallest Aβ-fiber neurons found (901 and 558 μm^2). Some very small Aβ-fiber neurons expressing SP have also been found in normal animals and have been reported to belong to the small group of nociceptive Aβ-fiber neurons in guinea pigs (Lawson et al., 1997). In the larger sample of unidentified DRG neurons, a small increase in medium-sized SP-immunoreactive neurons was seen in neuropathic animals compared with controls. Very few large DRG neurons expressed SP before and after CCI. In conclusion, if there is a phenotypic switch of Aβ-fiber neurons to express SP after CCI, it affects relatively small numbers of neurons.

Inverse relationship between NPY up-regulation and degree of thermal hyperalgesia

We found a strong inverse correlation between NPY expression in DRG neurons and the degree of thermal hyperalgesia in neuropathic mice. A previous study in the rat has found a similar relationship between galanin (another neuropeptide up-regulated in DRGs after nerve injury) and allodynia and a trend in the same direction for NPY (Shi et al., 1999). A correlation does not prove cause and effect, but one possible view of this relationship would be that up-regulation of NPY is an adaptive mechanism that counteracts the development of neuropathic pain and that insufficient NPY up-regulation leads to increased hyperalgesia. Indeed, many studies report antinociceptive actions of NPY in the rat spinal cord (see, e.g., Taiwo and Taylor, 2002; Sapunar et al., 2005), although this view has been challenged (Xu et al., 1999; Ossipov et al., 2002). Further studies will be needed to clarify whether NPY actually protects against the hyperalgesia induced by peripheral nerve injury.

LITERATURE CITED

Allen BJ, Li J, Menning PM, Rogers SD, Ghilardi J, Mantyh PW, Simone DA. 1999. Primary afferent fibers that contribute to increased substance P receptor internalization in the spinal cord after injury. J Neurophysiol 81:1379–1390.

Baba H, Doubell TP, Woolf CJ. 1999. Peripheral inflammation facilitates Aβ fiber-mediated synaptic input to the substantia gelatinosa of the adult rat spinal cord. J Neurosci 19:859–867.

Bennett GJ, Xie YK. 1988. A peripheral mononeuropathy in rat that produces disorders of pain sensation like those seen in man. Pain 33:87–107.

Brumovsky PR, Bergman E, Liu H-X, Hökfelt T, Villar MJ. 2004. Effect of a graded single constriction of the rat sciatic nerve on pain behavior and expression of immunoreactive NPY and NPY Y1 receptor in DRG neurons and spinal cord. Brain Res 1006:87–99.

Chaplan SR, Bach FW, Pogrel JW, Chung JM, Yaksh TL. 1994. Quantitative assessment of tactile allodynia in the rat paw. J Neurosci Methods 53:55–63.

The Journal of Comparative Neurology. DOI 10.1002/cne

336   R. RUSCHEWEYH ET AL.

Coggeshall RE, Lekan HA, Doubell TP, Allchorne A, Woolf CJ. 1997. Central changes in primary afferent fibers following peripheral nerve lesions. Neuroscience 77:1115–1122.

Corness J, Shi TJ, Xu ZQ, Brulet P, Hökfelt T. 1996. Influence of leukemia inhibitory factor on galanin/GMAP and neuropeptide Y expression in mouse primary sensory neurons after axotomy. Exp Brain Res 112:79–88.

Cuello AC, Galfre G, Milstein C. 1979. Detection of substance P in the central nervous system by a monoclonal antibody. Proc Natl Acad Sci U S A 76:3532–3536.

Dirajlal S, Pauers LE, Stucky CL. 2003. Differential response properties of IB₄-positive and -negative unmyelinated sensory neurons to protons and capsaicin. J Neurophysiol 89:513–524.

Dixon WJ. 1965. The up-and-down method for small samples. J Am Statist Assoc 60:967–978.

Djouhri L, Lawson SN. 2001. Increased conduction velocity of nociceptive primary afferent neurons during unilateral hindlimb inflammation in the anaesthetised guinea-pig. Neuroscience 102:669–679.

Dodt H-U, Zieglgänsberger W. 1990. Visualizing unstained neurons in living brain slices by infrared DIC-videomicroscopy. Brain Res 537:333–336.

Fang X, McMullan S, Lawson SN, Djouhri L. 2005. Electrophysiological differences between nociceptive and non-nociceptive dorsal root ganglion neurones in the rat in vivo. J Physiol 565:927–943.

Fang X, Djouhri L, McMullan S, Berry C, Waxman SG, Okuse K, Lawson SN. 2006. Intense isolectin-B4 binding in rat dorsal root ganglion neurons distinguishes C-fiber nociceptors with broad action potentials and high Nav1.9 expression. J Neurosci 26:7281–7292.

Fukuoka T, Tokunaga A, Kondo E, Miki K, Tachibana T, Noguchi K. 1998. Change in mRNAs for neuropeptides and the GABAₐ receptor in dorsal root ganglion neurons in a rat experimental neuropathic pain model. Pain 78:13–26.

Hammond DL, Ackerman L, Holdsworth R, Elzey B. 2004. Effects of spinal nerve ligation on immunohistochemically identified neurons in the L4 and L5 dorsal root ganglia of the rat. J Comp Neurol 475:575–589.

Hargreaves K, Dubner R, Brown F, Flores C, Joris J. 1988. A new and sensitive method for measuring thermal nociception in cutaneous hyperalgesia. Pain 32:77–88.

Harper AA, Lawson SN. 1985. Conduction velocity is related to morphological cell type in rat dorsal root ganglion neurones. J Physiol 359:31–46.

Honoré P, Rogers SD, Schwei MJ, Salak-Johnson JL, Luger NM, Sabino MC, Clohisy DR, Mantyh PW. 2000. Murine models of inflammatory, neuropathic and cancer pain each generates a unique set of neurochemical changes in the spinal cord and sensory neurons. Neuroscience 98:585–598.

Hunt SP, Mantyh PW. 2001. The molecular dynamics of pain control. Nat Rev Neurosci 2:83–91.

Julius D, Basbaum AI. 2001. Molecular mechanisms of nociception. Nature 413:203–210.

Koltzenburg M, Stucky CL, Lewin GR. 1997. Receptive properties of mouse sensory neurons innervating hairy skin. J Neurophysiol 78:1841–1850.

Lawson SN, Waddell PJ. 1991. Soma neurofilament immunoreactivity is related to cell size and fiber conduction velocity in rat primary sensory neurons. J Physiol 435:41–63.

Lawson SN, McCarthy PW, Prabhakar E. 1996. Electrophysiological properties of neurones with CGRP-like immunoreactivity in rat dorsal root ganglia. J Comp Neurol 365:355–366.

Lawson SN, Crepps BA, Perl ER. 1997. Relationship of substance P to afferent characteristics of dorsal root ganglion neurones in guinea-pig. J Physiol 505:177–191.

Lawson SN, Crepps B, Perl ER. 2002. Calcitonin gene-related peptide immunoreactivity and afferent receptive properties of dorsal root ganglion neurones in guinea-pigs. J Physiol 540:989–1002.

Ma W, Bisby MA. 1998a. Increase of preprotachykinin mRNA and substance P immunoreactivity in spared dorsal root ganglion neurons following partial sciatic nerve injury. Eur J Neurosci 10:2388–2399.

Ma W, Bisby MA. 1998b. Partial and complete sciatic nerve injuries induce similar increases of neuropeptide Y and vasoactive intestinal peptide immunoreactivities in primary sensory neurons and their central projections. Neuroscience 86:1217–1234.

Ma W, Bisby MA. 1998c. Increase of calcitonin gene-related peptide immunoreactivity in the axonal fibers of the gracile nuclei of adult and aged rats after complete and partial sciatic nerve injuries. Exp Neurol 152:137–149.

Marchand JE, Wurm WH, Kato T, Kream RM. 1994. Altered tachykinin expression by dorsal root ganglion neurons in a rat model of neuropathic pain. Pain 58:219–231.

McCarthy PW, Lawson SN. 1989. Cell type and conduction velocity of rat primary sensory neurons with substance P-like immunoreactivity. Neuroscience 28:745–753.

McCarthy PW, Lawson SN. 1990. Cell type and conduction velocity of rat primary sensory neurons with calcitonin gene-related peptide-like immunoreactivity. Neuroscience 34:623–632.

McCarthy PW, Lawson SN. 1997. Differing action potential shapes in rat dorsal root ganglion neurones related to their substance P and calcitonin gene-related peptide immunoreactivity. J Comp Neurol 388:541–549.

Noguchi K, Dubner R, De Leon M, Senba E, Ruda MA. 1994. Axotomy induces preprotachykinin gene expression in a subpopulation of dorsal root ganglion neurons. J Neurosci Res 37:596–603.

Noguchi K, Kawai Y, Fukuoka T, Senba E, Miki K. 1995. Substance P induced by peripheral nerve injury in primary afferent sensory neurons and its effect on dorsal column nucleus neurons. J Neurosci 15:7633–7643.

Ossipov MH, Zhang E-T, Carvajal C, Gardell L, Quirion R, Dumont Y, Lai J, Porreca F. 2002. Selective mediation of nerve injury-induced tactile hypersensitivity by neuropeptide Y. J Neurosci 22:9858–9867.

Sapunar D, Modric-Jednacak K, Grkovic I, Michalkiewicz M, Hogan H. 2005. Effect of peripheral axotomy on pain-related behavior and dorsal root ganglion neurons excitability in NPY transgenic rats. Brain Res 1063:48–58.

Schäfers M, Geis C, Svensson CI, Luo ZD, Sommer C. 2003. Selective increase of tumour necrosis factor-alpha in injured and spared myelinated primary afferents after chronic constrictive injury of rat sciatic nerve. Eur J Neurosci 17:791–804.

Schoffnegger D, Heinke B, Sommer C, Sandkühler J. 2006. Physiological properties of spinal lamina II GABAergic neurons in mice following peripheral nerve injury. J Physiol 577:869–878.

Shehab SA, Spike RC, Todd AJ. 2003. Evidence against cholera toxin B subunit as a reliable tracer for sprouting of primary afferents following peripheral nerve injury. Brain Res 964:218–227.

Shi T-JS, Gui J-G, Meyerson BA, Linderoth B, Hökfelt T. 1999. Regulation of galanin and neuropeptide Y in dorsal root ganglia and dorsal horn in rat mononeuropathic models: possible relation to tactile hypersensitivity. Neuroscience 93:741–757.

Shi T-JS, Tandrup T, Bergman E, Xu Z-Q, Ulfhake B, Hökfelt T. 2001. Effect of peripheral nerve injury on dorsal root ganglion neurons in the C57 BL/6J mouse: marked changes both in cell numbers and neuropeptide expression. Neuroscience 105:249–263.

Sommer C, Schäfers M. 1998. Painful mononeuropathy in C57BL/Wld mice with delayed wallerian degeneration: differential effects of cytokine production and nerve regeneration on thermal and mechanical hypersensitivity. Brain Res 784:154–162.

Taiwo OB, Taylor BK. 2002. Antihyperalgesic effects of intrathecal neuropeptide Y during inflammation are mediated by Y1 receptors. Pain 96:353–363.

Tandrup T, Woolf CJ, Coggeshall RE. 2000. Delayed loss of small dorsal root ganglion cells after transection of the rat sciatic nerve. J Comp Neurol 422:172–180.

Tie-Jun SS, Xu Z, Hökfelt T. 2001. The expression of calcitonin gene-related peptide in dorsal horn neurons of the mouse lumbar spinal cord. Neuroreport 12:739–743.

Wakisaka S, Kajander KC, Bennett GJ. 1992. Effects of peripheral nerve injuries and tissue inflammation on the levels of neuropeptide Y-like immunoreactivity in rat primary afferent neurons. Brain Res 598:349–352.

Wang H, Rivero-Melián C, Robertson B, Grant G. 1994. Transganglionic transport and binding of the isolectin B4 from *Griffonia simplicifolia* I in rat primary sensory neurons. Neuroscience 62:539–551.

Wang R, Guo W, Ossipov MH, Vanderah TW, Porreca F, Lai J. 2003. Glial cell line-derived neurotrophic factor normalizes neurochemical changes in injured dorsal root ganglion neurons and prevents the expression of experimental neuropathic pain. Neuroscience 121:815–824.

Woolf CJ. 2004. Dissecting out mechanisms responsible for peripheral neuropathic pain: implications for diagnosis and therapy. Life Sci 74:2605–2610.

Xu IS, Hao J-X, Xu X-J, Hökfelt T, Wiesenfeld-Hallin Z. 1999. The effect of intrathecal selective agonists of Y₁ and Y₂ neuropeptide Y receptors on the flexor reflex in normal and axotomized rats. Brain Res 833:251–257.

Zieglgänsberger W, Berthele A, Tölle TR. 2005. Understanding neuropathic pain. CNS Spectr 10:298–308.